9. Task 9 Development of Hydrogen Transportation and Storage Technology

9.1 Development of Liquid Hydrogen Transportation and Storage Facilities

9.1.1 R&D Goals

Continuing from last year, we conduct insulation performance tests on two specimens and low-temperature strength tests on one specimen, to develop a design database on thermal insulation structure for large-scale storage to be used for liquid hydrogen tankers and land-based liquid hydrogen tanks. In the thermal insulation tests, a thermal flow meter is attached to the specimens to measure the heat flow and comparison with conventional evaporation method was made.

Small-capacity liquid hydrogen transportation and storage system is studied for the purpose of supplying hydrogen to hydrogen stations for fuel cell powered vehicle. In the study applicable laws and standards for liquid hydrogen transportation and storage tank (container tank) are investigated, and conceptual design of tanks with capacity of $30m^3$ and $15m^3$ are produced. Preliminary study is also started on sloshing (splashing) of liquid hydrogen that occurs during transportation.

We study a medium-sized hydrogen supply chain for marine transportation system, which is about halfway between large-scale and small-scale transportation and storage. A marine transportation system is studied with Tokyo Bay area as a model case.

9.1.2 Results FY2001

9.1.2.1 Thermal insulation test with thermal insulation structure specimens

(1) Design and production of specimens for insulation test

As specimens for thermal insulation test, a perlite vacuum insulation structure specimen (for land use) and a vacuum panel type insulation structure (for tanker) were designed and produced.

(1.1) Powder vacuum insulation structure specimen (for tank)

Powder vacuum insulation structure specimen (dimensions: 1,000mm diameter x 250mm thickness, filler material: microsphere (glass microscopic hollow powder, average grain diameter: 50μm), degree of internal vacuum: 0.1Pa or less) was designed and produced to conduct a liquid hydrogen test. Fig.9.1.2-1 shows SEM image of micro sphere.

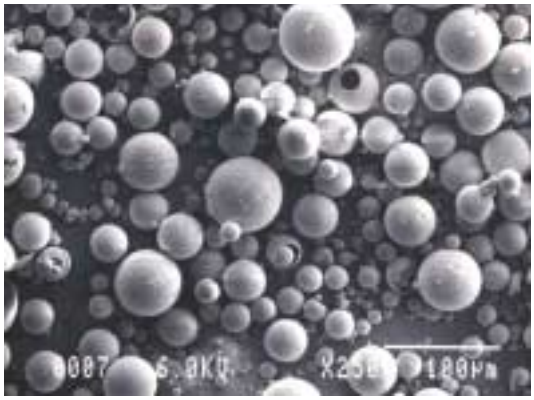

Fig.9.1.2-1 SEM image of microsphere

Fig. 9.1.2-2 Panel vacuum type insulation structure specimen

(1.2) Panel vacuum type insulation structure specimen (for tanker)

A panel vacuum type insulation structure specimen (dimensions: 1,019mm diameter x 200mm thickness, filler core material: polyurethane foam, outer jacket material: SUS (thickness: 0.5mm and 0.3mm), degree internal vacuum: 0.1Pa or less) was designed and produced to conduct a liquid hydrogen test. Fig. 9.1.2-2 shows Panel vacuum type insulation structure specimen.

(2) Results of thermal insulation tests

We reviewed the results of last year's tests on solid-vacuum insulation structure specimen and perlite atmospheric pressure insulation structure specimen and conducted additional studies. We then conducted an outline study on the test results on this year's vacuum panel type insulation structure and perlite vacuum insulation structure specimens.

(2.1) Study on solid-vacuum insulation structure specimen (urethane foam with support, for tanker)

Side heat input was evaluated from the temperature difference between position of specimens with 780mm diameter and 1,180mm diameter to correct the heat input into the liquid hydrogen container for measurement. The results indicated that actual thermal conductivity improved by 11% over the value of 5.6mW/m-K given in last year's Study Report. With the above-mentioned side heat input included in the conditions, a detailed temperature distribution analysis was conducted using a general-purpose code NASTRAN to study the effects on insulation properties of the support structure.

(2.2) Study on perlite atmospheric pressure insulation structure specimen (for tank)

For the perlite atmospheric pressure insulation structure specimen (dimensions:

1,100mm diameter x 200mm thickness, filler material: perlite, filler gas: helium gas at atmospheric pressure), actual measurement data of gap part (20mm average) was input for recalculations using a general-purpose code PHOENICS. The results indicated that thermal conductivity of the perlite part was about 3 times larger (100mW/m-K) than for the case using nitrogen filler gas. Natural convection of gas was confirmed in the gap part, verifying that effect of helium thermal conductivity (70mW/m-K@80K) was large.

(2.3) Study on perlite vacuum insulation structure specimen (for tank)

Test on perlite vacuum insulation structure specimen was started with internal vacuum set at 10Pa, and thermal conductivity in a quasi-steady state was about 20mW/m-K. The test was aborted as liquid hydrogen supply could not keep up during the test. We plan to conduct a retest next year in a steady state.

(2.4) Study on panel vacuum type insulation structure (for tanker)

For this test a heat flux sensor (thermopile type) was attached to the high-temperature face of the specimen to compare with thermal conductivity equivalent to amount of evaporation. The measured thermal conductivity was 5.1mW/m-K. Fig. 9.1.2-3 shows Thermal insulation test apparatus with panel vacuum test insulation structure specimen.

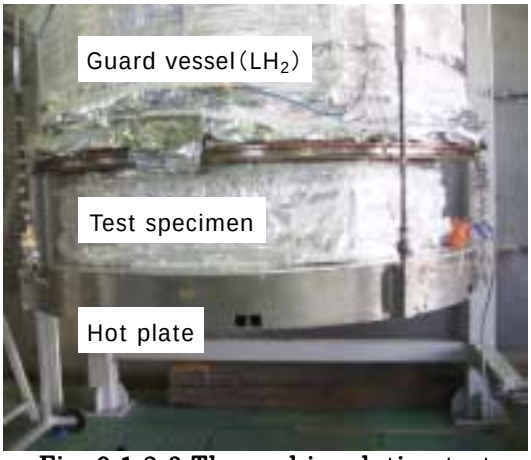

Fig. 9.1.2-3 Thermal insulation test apparatus with panel vacuum type insulation structure specimen

9.1.2.2 Low-temperature strength test

Bottom insulation material for land-based storage tank and the lightweight concrete specimen (100mm diameter x 50mm height) were designed and produced, and strength tests at normal temperature and at low temperatures in liquid nitrogen and liquid hydrogen were conducted. Compressive strength in liquid hydrogen was 93.2~130.6N/mm^2, increasing by 3.1 to 4.4 times the strength at normal temperature (30N/mm^2). Compressive strength at low temperatures tended to vary, but strength tended to increase as the temperature dropped. Fig.9.1.2-4 shows Strength test apparatus with the lightweight concrete specimen. Fig.9.1.2-5 shows Relationship between the temperature and the increase of compressive strength.

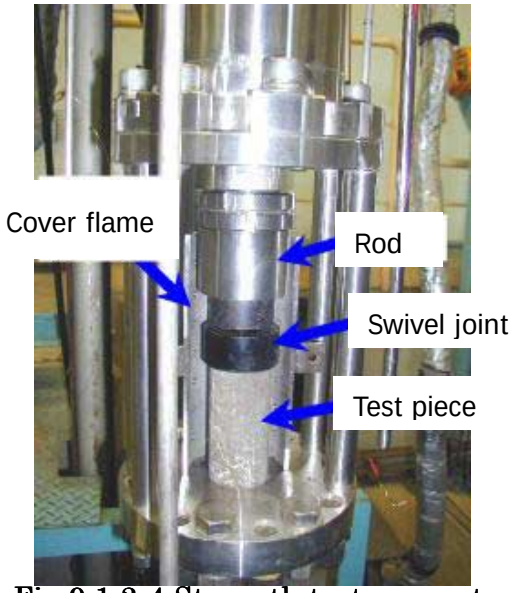

Fig.9.1.2-4 Strength test apparatus with the lightweight concrete specimen

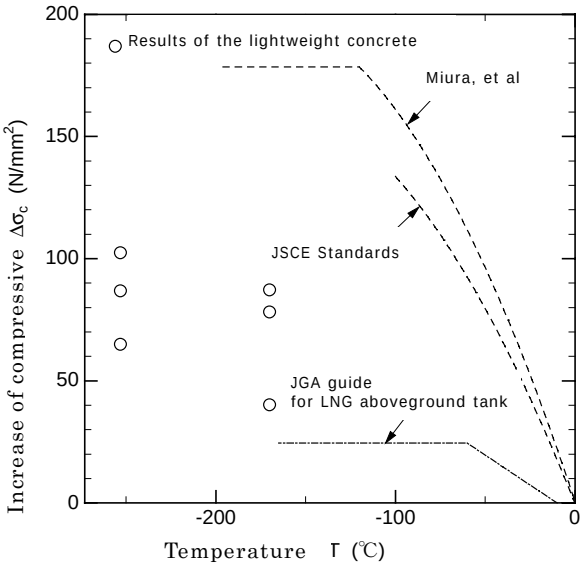

Fig.9.1.2-5 Relationship between the temperature and the increase of compressive strength

9.1.2.3 Study on small-capacity liquid hydrogen transportation and storage system

(1) Legal regulations for transporting liquid hydrogen and investigation on standards on transportation and storage tanks

We investigated the High Pressure Gas Safety Law (Container Safety Regulations, General High Pressure Gas Safety Regulations), Vehicles Act (Safety Standards), Nippon Kaiji Kyokai (NK) Regulations (Marine Container Regulations, Marine Container Inspection Guideline), etc. to reflect on trial design of tank.

(2) Conceptual design of small liquid hydrogen tank for transportation and storage (container tank)

Inner tank support methods were compared for liquid hydrogen tank for transportation and storage with capacity of 30m^3 and 15m^3, and trial design (strength calculation, heat input calculation) was conducted for tank with a target thermal insulation (BOG) of 0.5%/day. Fig.9.1.2-6 shows Conceptual design of small liquid hydrogen tank.

(3) Preliminary study on thermal flow by sloshing during transportation in liquid hydrogen container

We estimated the splashing energy from sloshing caused by disturbance such as acceleration during transportation and found that the heat converted from this

energy was small compared to the steady heat input. We also studied the splashing on free surface of liquid hydrogen and other cryogenic liquids and confirmed that splashing on free surface of liquid hydrogen tended to be larger than others.

(4) Pressure rise and stratification phenomenon in liquid hydrogen container tank

We created a simplified model in which liquid and gas phases were integrated to estimate the pressure rise with amount of condensation in gas phase as parameter.

Also, preliminary study was conducted on stratification phenomenon, which occurs in the upper portion of liquids in association with pressure rise in the tank.

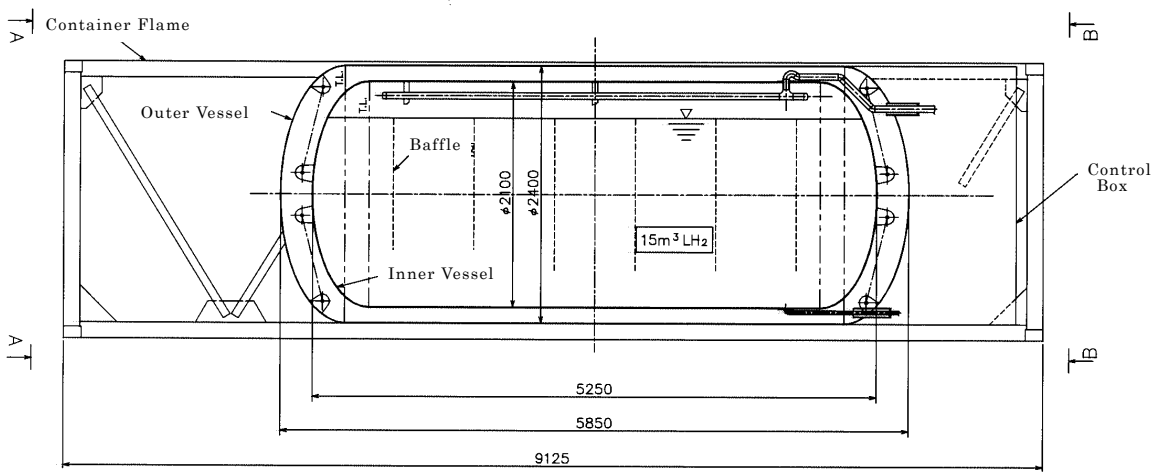

Fig.9.1.2-6 Conceptual design of small liquid hydrogen tank

Principal specifications

Type	Double-hull horizontal cylindrical container
Capacity	$30m^3/15m^3$
Insulation system	Vacuum multilayer insulation
Degree of vacuum	10^{-2}Pa
Insulation performance (evaporation rate)	
	0.5%/day or less [target performance]
Principal dimensions	Inner tank inner diameter:φ2,100 mm
	Outer tank inner diameter:φ2,400 mm

Liquid hydrogen container tank ($15m^3$) and principal specifications

9.1.2.4 Study of medium-sized liquid hydrogen supply chain

With Tokyo Bay coastal area as the model, we studied a marine transportation system with tank capacity of transport barge as parameters ($90m^3$, $250m^3$, $480m^3$), for medium-sized liquid hydrogen supply chain.

9.1.3 Subject in future

We plan to conduct insulation performance tests on two specimens (microsphere, etc.) and low-temperature strength tests on GFRP, and review the results of each conceptual design for tankers and land-based tanks that was conducted in Phase 1, based on results of elemental tests conducted so far.

As research and development on small-capacity liquid hydrogen transportation and storage system, we also plan to develop and produce a liquid hydrogen transportation and storage tank (container tank) and conduct preliminary performance tests using liquid nitrogen. In small-capacity systems, we plan to conduct feasibility studies and equipment review on other modes of hydrogen transportation and storage (hydrogen-absorbing alloy, chemical hydride, pipeline, etc.) to identify technical tasks and evaluate energy efficiency, cost effectiveness, etc., to verify that liquid hydrogen is a promising transportation and storage mode.

9.2 Development of Devices for Common Use

9.2.1 R&D Goals

This fiscal year, we select a theme related to small capacity transportation and storage of hydrogen assuming hydrogen stations. A test equipment was newly made for testing hydrostatic bearing, which is a non-contact bearing similar to magnetic bearing and considered for application in small-scale liquid hydrogen pumps, and bearing evaluation by rotation test is conducted.

Then, we examine the required specifications for small-scale liquid hydrogen pumps to be used in liquid hydrogen stations and carry out the basic plans for pump specifications, motor specifications and bearing specifications according to the fixed basic specifications.

Also, as part of equipment development for liquid hydrogen stations, we conduct studies on recovery and utilization of boil-off hydrogen that is generated during storage of liquid hydrogen. Specifically, the energy balance related to utilization is reviewed, including re-liquefaction of recovered hydrogen, storage of high-pressure gas, fuel cell generation, etc.

9.2.2 Results FY2001

9.2.2.2 Evaluation tests for hydrostatic bearing

(1) Design of hydrostatic bearing

In order to obtain basic data on hydrostatic bearings to be used in the bearing system of liquid hydrogen pumps, test equipment for testing hydrostatic bearing were designed and made. For the radial bearing pad, three types of bearing pad were designed and made: ①fluid hydrostatic bearing, ②hydrogen gas hydrostatic bearing and ③fluid foil hydrostatic bearing. For the thrust bearing pad, ④hydrogen gas hydrostatic bearing was designed and made for use in all three pad types. Specifications are listed in Table 9.2.2-1

Table 9.2.2-1 Design specifications

Type / Item	Radial bearing			Thrust bearing
	①Fluid hydrostatic bearing	②Hydrogen gas hydrostatic bearing	③Fluid foil hydrostatic bearing	④Hydrogen gas hydrostatic bearing
Bearing inner diameter [mm]	φ20	φ20	φ20	Thrust inner diameter: φ42
Bearing width [mm]	20	20	20	Thrust outer diameter:φ63
Inlet configuration	φ1mm×4 with recess	φ1mm×8× 2 rows	Not needed	φ1mm×18
Inlet pressure [MPa]	0.5,1.0,2.0	1.5	0.2	0.3
Working fluid	Liquid hydrogen	Hydrogen gas	Liquid hydrogen	Hydrogen gas
Radial gap [μm]	30	20	200 (Movable range)	150 (Movable range)

(2) Evaluation test

We used a bearing test equipment which simulates operation of actual pumps to conduct a rotation performance test with gas and liquid hydrogen externally supplied. Performance data at a rated speed of 20,000 rpm was acquired.

Cross section of the prototype test equipment is shown in Fig.9.2.2-1. This figure shows a typical configuration with a fluid hydrostatic bearing built in, and three types of test can be conducted by changing the bearing pad unit. As a representative bearing pad, photograph of a foil bearing unit is displayed in Fig.9. 2.2-2.

Photographs of setup for foil bearing test is shown in Figure9.2.2-3. Test equipment was fixed on a mount and connected to the piping system on the test equipment side, and tests were conducted with the entire equipment covered with thermal insulation material.

(3) Performance evaluation test

[Foil bearing test]

Foil bearing unit was filled with LH_2 and rotor shaft rotation was gradually increased. The rotor shaft lifted up at around 8,000rpm and steady operation up to a maximum rotation of 58,000rpm was confirmed. The shaft lifted up again after it touched down due to an error in feed pressure control, and steady operation at around 20,000rpm was confirmed. It was confirmed that shaft vibration could be contained within 10μmp-p. Vibration during the rotation test is shown in Fig.9.2 2-4.

[Fluid hydrostatic bearing test]

LH_2 was gradually supplied to the radial bearing unit and it was confirmed that the rotor shaft lifted up in the center of the radial shaft at around 1.0MPa. Rotor shaft rotation was gradually increased to monitor rotational vibration and the rotor shaft started to rotate after about 250 seconds into the test. When rotation rose to around 50,000rpm, rotor shaft and bearing pad touched, causing rotation to stop immediately.

(4) Summary of the evaluation tests

① In radial bearing design, rotor shaft diameter was set at φ20mm to calculate the bearing performance for fluid hydrostatic bearing, hydrogen gas hydrostatic bearing and fluid foil hydrostatic bearing. Optimum values for supply pressure of lubricating fluid and bearing radial gap were calculated by parameter survey.

② In thrust bearing design, hydrogen gas hydrostatic bearing system was selected, which was common to all three types of radial bearing. Although thrust was applied from only one direction, thrust bearing with the same specifications were also placed on the non-load side and thrust reactive force were applied as necessary, for stability control against disturbance.

③ It was confirmed that thrust bearing could be held at a prescribed position. Its rigidity was also confirmed by hand pushing to be sufficient against the design load of 73N.

④ In foil bearing test it was confirmed that rotor shaft lifted up normally between 6,000rpm and 8,000rpm and a stable increase up to a maximum rotation of 58,000rpm was confirmed. In steady operation at 20,000rpm it was confirmed that rotor shaft vibration was stable, within 10μmp-p at maximum.

⑤ In overhaul after the foil bearing test, peeling off of coating was found on the rotor shaft side, caused by contact between rotor shaft and foil plate. The cause seems to be the foil plate scratching the coating due to roughness of the foil plate surface. In general, this should not be a problem in ordinary design as coating will be applied to the foil side. (In the case of foil bearing, coating was applied to the rotor shaft side as a special measure to provide commonality among three types of bearing pad.)

⑥ In hydrogen gas hydrostatic bearing test, it was confirmed that radial bearing lifted up normally and could be held at the center of bearing pad. As turbine supply pressure was gradually increased, rotor shaft started to rotate after about 250 seconds. After passing the primary critical speed of about 14,000rpm, rotor shaft and bearing pad touched at around 50,000rpm and rotation stopped immediately. As design primary critical speed is around 30,000rpm and secondary critical speed is around 40,000rpm, cause of the failure is estimated to be that rigidity of the bearing was not up to the designed level.

9.2.2.2 Design of compact liquid hydrogen pumps for hydrogen stations

Required specifications for pumps to be used in liquid hydrogen stations were fixed as listed in Table 9.2.2-2, based on research of specifications for pumps used in existing liquid hydrogen pump and automobile LNG stations.

Table 9.2.2-2 Liquid hydrogen pump specifications

Parameter	Basic Specification	Unit
Flow Rate	3.6	m^3/h
Pump Head	160	m
Ns Value	109	(m^3/h,m,rpm)
Rotation Speed	20,000	rpm

(1) Review of pump impeller specifications

After conducting the basic design based on the above pump specifications, closed centrifugal pump with a guide vane was selected. It was found that specifications could be achieved with 5 blades, impeller outer diameter of 60mm and one stage.

(2) Review of motor specifications

After conducting an outline review, an AC motor with two poles, rated power of 0.5kW and source voltage of 200V was selected. Rough dimensions were: For rotator, inner diameter =φ25mm, outer diameter =φ63.8mm, width = 55mm; For stator, inner diameter =φ65mm, outer diameter =φ135mm, width = 150mm. When selecting

magnetic material and insulation material, attention should be given to cryogenic characteristics and brittleness against hydrogen.

(3) Study of bearing specifications

When using an electric motor for driving the pump, problems arise such as increase in load capacity on bearing and instability in rotating system associated with drop in natural frequency of spring-mass system, which are caused by increase in the weight of rotor shaft iron core. Therefore, a method to support the bearing with elastic material should also be considered in bearing design.

9.2.2.3 Review of technology to recover boil-off hydrogen gas in liquid hydrogen station

Re-liquefaction was reviewed as a technology to recover boil-off hydrogen gas and it was found to be very inefficient, as a re-liquefaction unit requires three times the total power consumption of the entire hydrogen station facility. On the other hand, it was found that boil-off hydrogen gas, when used as fuel for fuel cells, yielded sufficient power to cover power consumption for the entire station. It was also found that it would be effective to recover the boil-off gas that is generated when liquid hydrogen is fed to automobiles, store it in high-pressure tank using hydrogen compressor, and supply to high pressure hydrogen vehicles or hydrogen-absorbing alloy vehicles.

9.2.3 Subject in future

① We will conduct detail design and production of compact general-purpose liquid hydrogen pump, which is applicable to liquid hydrogen station.

② We will conduct detail design, production and evaluation of a QD that can recover the boil-off gas that is emitted when liquid hydrogen is supplied.

③ We will modify the hydrogen gas hydrostatic bearing test equipment to conduct validation tests, using as parameters bearing conditions that reflect basic motor specifications.

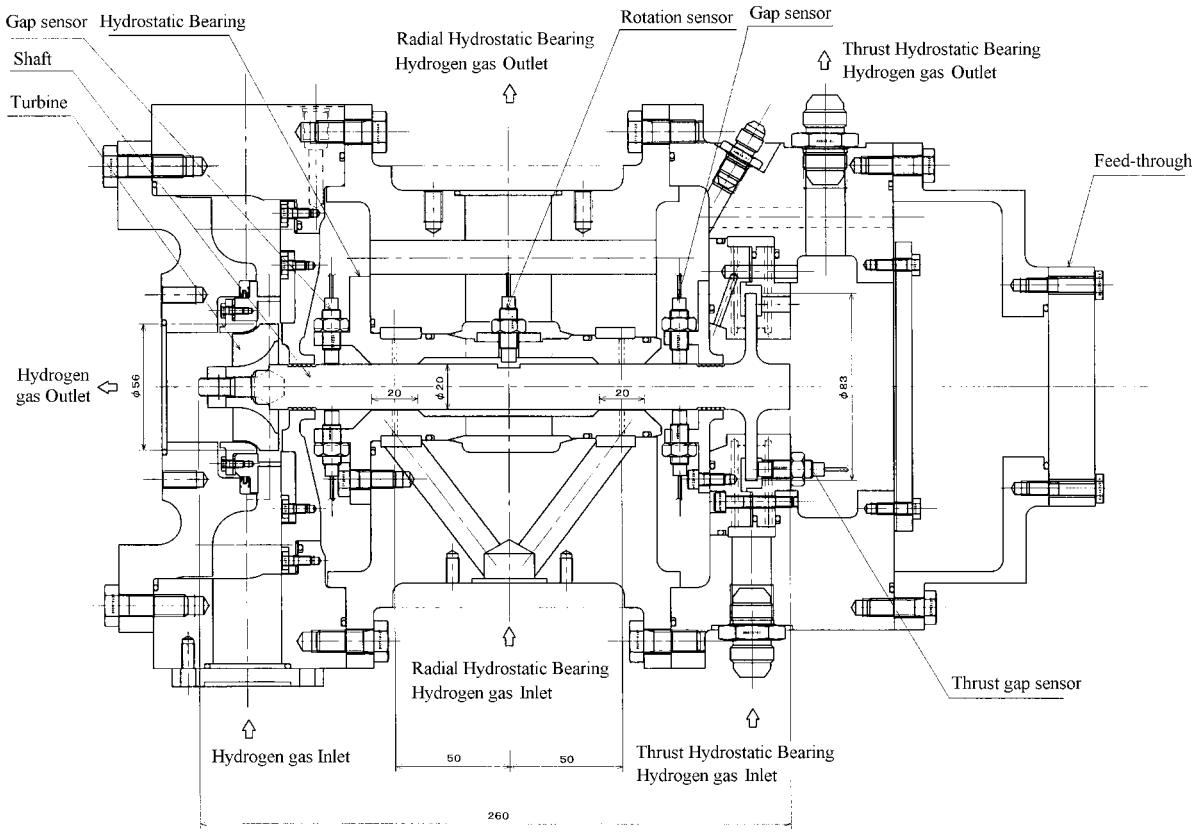

Fig9.2.2-1 The cross section of the test equipment

Fig9.2.2-2 The photograph of Foil Bearing

Fig9.2.2-3 The photograph of Foil Bearing in test conditions

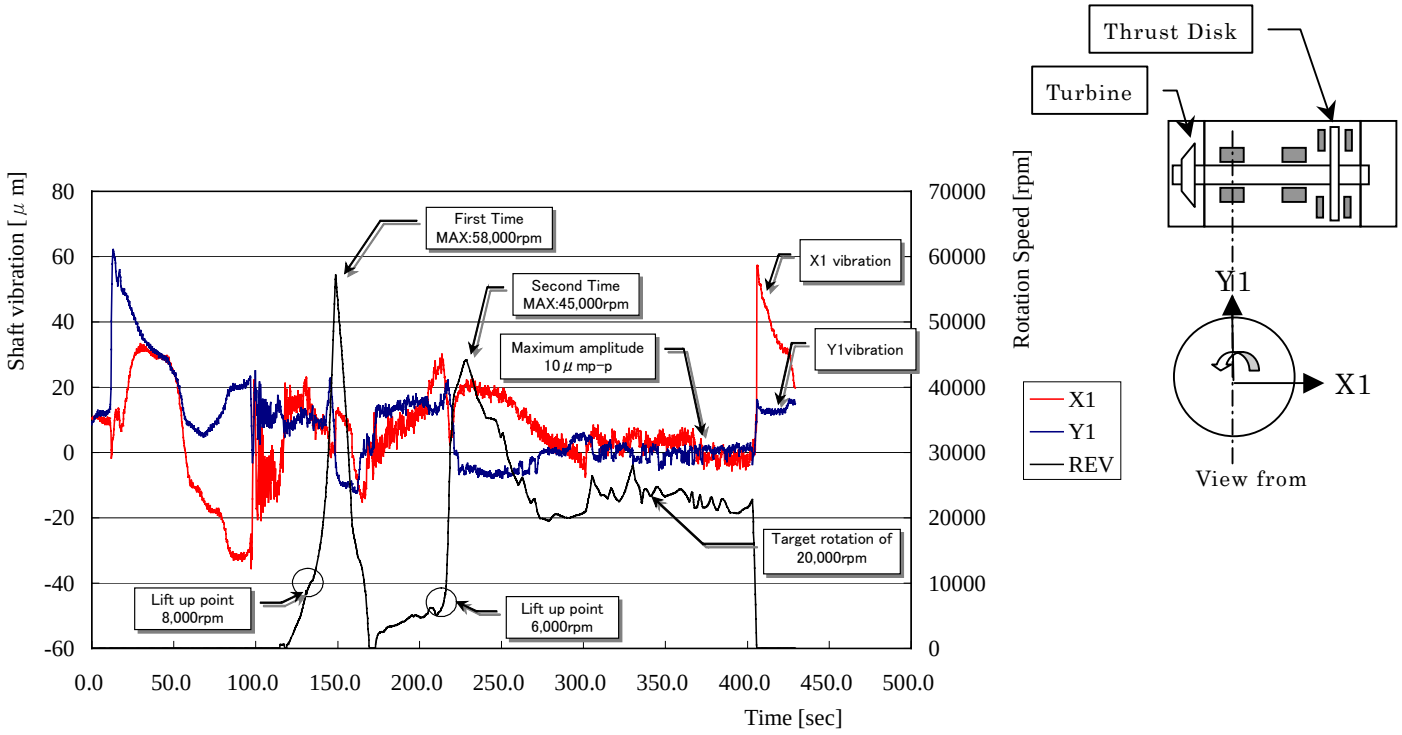

(1)Shaft vibration (Turbine side)

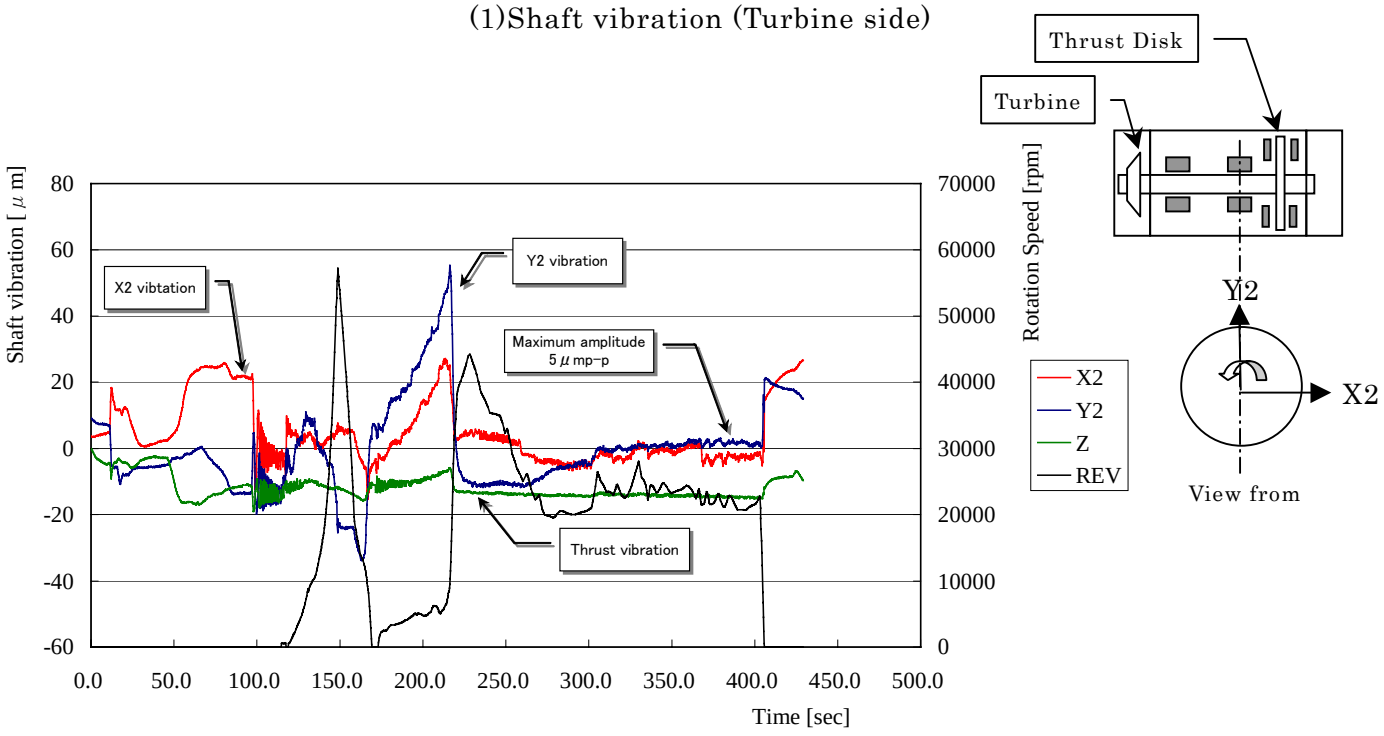

(2)Shaft vibration (Thrust disk side) and Thrust vibration

Fig 9.2.2-4 Shaft vibration in rotation test of Foil Bearing

9.3 Conceptual Design of Hydrogen Liquefaction Facilities

9.3.1 R&D Goals

In the research and development plan of WE-NET Phase 2, we decided to work on development items assuming automobile hydrogen stations in coordination with development of fuel cell powered vehicles, in parallel with development of large-scale use of hydrogen, for gradual introduction of hydrogen energy. In Task 9-3, we are working on development of hydrogen liquefaction machine with a relatively small capacity of 30 ton/day or less, in preparation for the validation phase for automobile hydrogen stations, which is scheduled to start in Phase 3.This fiscal year, we study hydrogen expansion turbines for power recovery and power reduction in hydrogen liquefaction machine by utilizing the cryogenic heat of LNG for the purpose of reducing the compression power in hydrogen compressors, which we have been reviewing.

9.3.2 Results FY2001

9.3.2.1 Study of power recovery technology using hydrogen expansion turbine

For a relatively small hydrogen liquefaction machine to be used in automobile hydrogen stations, we conducted an outline study on the expansion turbine for power recovery. The expansion turbine extracts hydrogen gas from the high-pressure hydrogen gas line in the liquefaction cycle and expands it to recover power before returning it to the low-pressure line. The recovered power is intended to reduce the required power for the liquefaction compressor.

We decided to use the expansion turbines on the high temperature side and low temperature side of the hydrogen liquefaction machine shown in Figure 9.3.2-1, which had also been selected for 300t/d large scale hydrogen liquefaction facility in Phase 1.

Temperature and pressure conditions for the hydrogen expansion turbine were set as same as for the 300t/d facility, and flow rate was reduced in proportion to the amount of hydrogen liquefaction that was used as liquefaction capacity in this case study. Three cases of liquefaction capacity were studied: 1t/d, 5t/d and 10t/d.

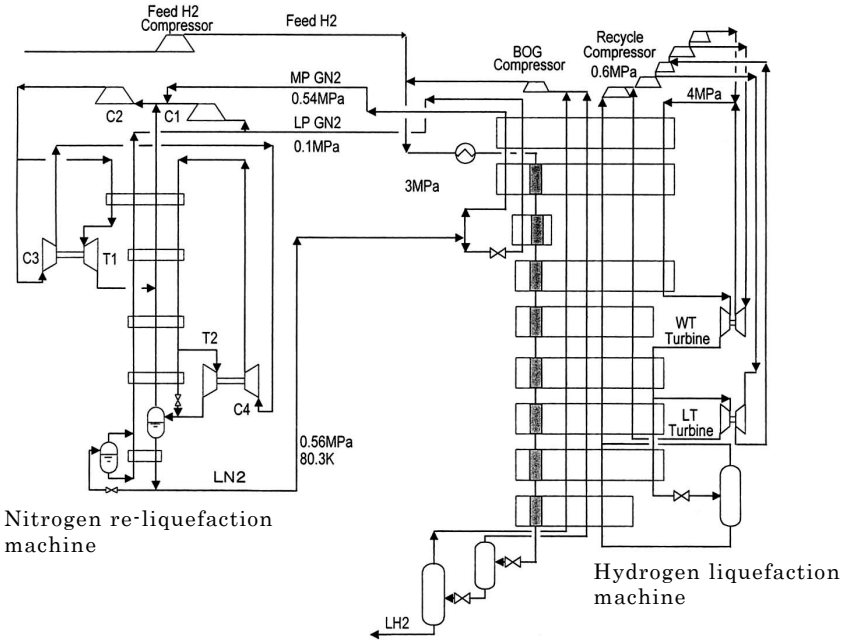

Figure 9.3.2-1. Process flow of hydrogen liquefaction machine

(1) Study of rough outline of centrifugal turbo-type hydrogen expansion turbine

In this study we selected radial turbine as expansion turbine for power recovery, which is a centrifugal type expansion turbine as shown in Figures 9.3.2-2 and 9.3.2-3. With this type, gas is entered through the inlet pipe and passes the scroll, then is expanded and accelerated through the nozzle to have a circular component in the circumferential direction, and fed into the rotor blades.

Gas is further expanded in the rotor blades and direction of the flow is changed from radial to axial, and discharged through the outlet pipe. As gas temperature drops due to adiabatic expansion, gas energy can also be recovered through rotor blades as shaft power.

In this study, three-dimensional rotor blades were reviewed with the aim to reduce the flow loss in the rotor blades and improve the efficiency of the expansion turbine. By warping the blades in the height direction as shown in Fig. 9.3.2-3, three-dimensional rotor blades can reduce the secondary flow loss (loss caused by a flow that occurs perpendicularly to the flow passage).

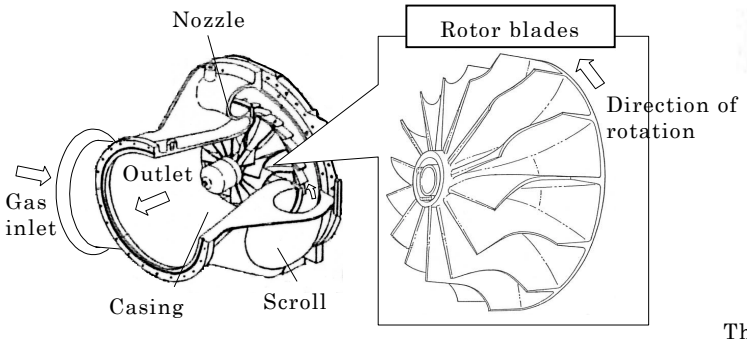

Fig.9.3.2-2. Rough outline of centrifugal turbo-type hydrogen expansion turbine

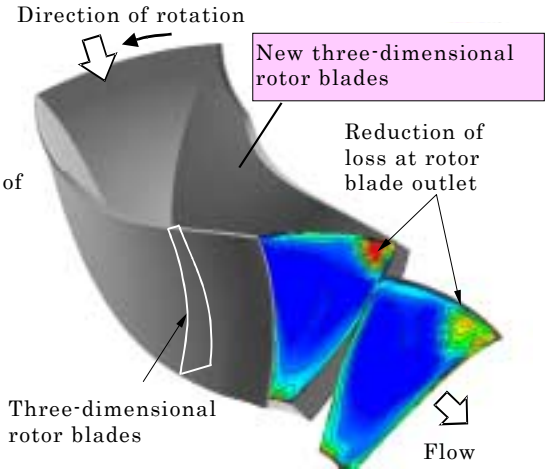

Fig. 9.3.2-3. Shape of rotor blades in centrifugal turbo-type hydrogen expansion turbine

Results of study on primary dimensions, power and efficiency for the rotor blades of the above-mentioned centrifugal turbo type hydrogen expansion turbine are listed in Table 9.3.2-1, with liquefaction capacity of hydrogen liquefaction facility as a parameter. Outer diameter of rotor blades becomes smaller as liquefaction quantity decreases.

Under the assumptions for this study, outer diameter of rotor blades was under 40mm for 5t/d turbine on high temperature side as well as for 1t/d turbine on high and low temperature sides, which are smaller than generally used centrifugal turbo type hydrogen expansion turbines.

There is a possibility here that effects of leakage flow may relatively increase in the clearance between rotor blades and casing. Therefore, there is a possibility that actual performance may be lower than the estimated performance based on calculation (Denoted by (*) in Table 9.3.2-1.)

As temperature and pressure conditions are constant in this study and flow rate is proportional to the liquefaction quantity, power output of the expansion turbine will be proportional to the product of efficiency and flow rate. From the above results, the efficiency of the expansion turbine is estimated to decrease as liquefaction quantity decreases. On high temperature side of 5t/d turbine and on high and low temperature sides of 1t/d, actual efficiency can be estimated to be lower than the results obtained by the above calculations.

Thus, in this study on power recovery with centrifugal turbo type turbine using the temperature and pressure conditions for 300t/d, there is a possibility that liquefaction quantity may decrease and the power to be recovered by may decrease

relative to the power required for liquefaction.

As shown in the results of outline study, coupling/tie-in with the hydrogen compressor, to which recovered power is supplied, is expected to be very difficult to achieve technical viability with gear systems, as turbine speed exceeds 100,000rpm. Therefore, power recovery by uniaxial direct coupling with the hydrogen compressor seems to be the realistic solution under the power recovery conditions for expansion turbine.

Table 9.3.2-1. Results of Study on Rough Outline of the Expansion Turbine

			10ton/day	5ton/day	1ton/day
High temperature expansion turbine WT	Dimensions	Width of rotor blade outlet b3(mm)	3.6	2.5	1.1
		Outer diameter of rotor blades D3(mm)	43.5	30.8	13.9
		Outer diameter of rotor blade outlet D4T(mm)	31.5	22.3	10.0
		Inner diameter of rotor blade outlet D4R(mm)	12.8	9.1	4.1
	Speed of rotation(rpm)		198128	279525	621078
	Output power(KW)		104	51	10
	Efficiency(−)		0.815	0.802(＊)	0.766(＊)
Low temperature expansion turbine LT	Dimensions	Width of rotor blade outlet b3(mm)	4.9	3.5	1.6
		Outer diameter of rotor blades D3(mm)	60.1	42.6	19.2
		Outer diameter of rotor blade outlet D4T(mm)	43.5	30.9	13.9
		Inner diameter of rotor blade outlet D4R(mm)	17.7	12.6	5.7
	Speed of rotation(rpm)		122935	173260	385091
	Output power(KW)		74	36	7
	Efficiency(−)		0.828	0.817	0.785(＊)

(2) Study of thrust force of a centrifugal turbo-type hydrogen expansion turbine

The expansion turbine for power recovery has an inlet pressure of 4.05MPa on high temperature side and 16.8MPa on low temperature side, and therefore thrust force on turbine is expected to be large. Since thrust force affects the viability of the shaft, it is necessary to consider reducing it. In this study we conducted a study on the thrust force working on the turbine and measures to reduce it using balance rings, based on results of the above-mentioned form review and operating conditions of the turbine. As shown in Figure 9.3.2-4, turbine thrust works in the direction of hydrogen outflow at the turbine outlet. In a hydrogen liquefaction facility of 10t/d, thrust force is about 60kgf for high temperature expansion turbine and about 50kgf for low temperature expansion turbine.

Thus, we conducted a study on thrust control with balance rings. Figure 9.3.2-5 shows results of study on thrust control in expansion turbine on high-temperature

side in a 10t/d liquefaction machine. Results indicated that it was possible to reduce the above thrust force by optimizing the diameter of balance rings.

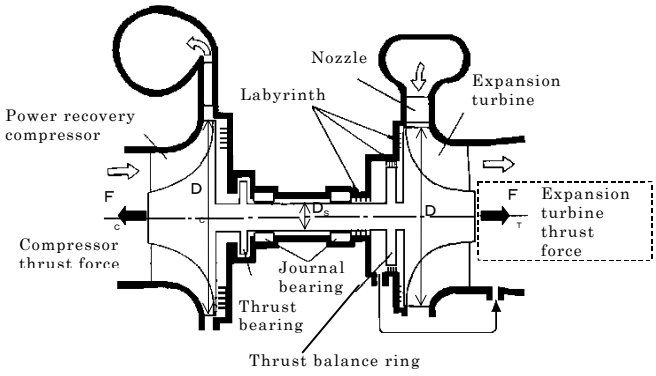

Figure 9.3.2-4. Thrust force working on the expansion turbine

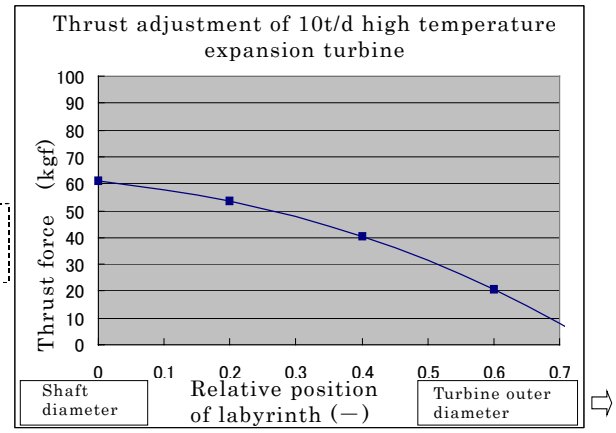

Figure 9.3.2-5. Results of study on thrust force (high temperature expansion turbine)

9.3.2.2 Study on reduction of required power for hydrogen liquefaction using LNG cooling

We assumed a case where hydrogen is produced from natural gas and liquefied at or near an LNG base, and conducted a study on required power for hydrogen liquefaction using LNG cooling. It was confirmed that substantial reduction of power would be possible.

(1) Hydrogen liquefaction power by conventional methods

Results of past studies on required power for liquefaction by conventional methods for 1t/d, 10t/d and 30t/d liquefaction machines are summarized in Table 9.3.2-2. Also, an outline flow of hydrogen liquefaction machine is shown in Figure 9.3.2-6.

Table 9.3.2-2. Power required for hydrogen liquefaction by conventional method

Scale of supply	t/d	1	10	30
Number of hydrogen liquefaction machines		1	1	1
Hydrogen expansion turbine		2	3	3
Hydrogen compressor		3(Reciprocating type)	3(Reciprocating type)	3(Reciprocating type)
Nitrogen re-liquefaction cycle				
Number of nitrogen re-liquefaction machines		1	1	1
Expansion turbine		1	1	2
Power recovery		No	Yes	Yes
Required power				
Raw hydrogen compressor	MW	0.0850	0.850	2.550
Low pressure recycle compressor	MW	0.0133	0.133	0.408
High pressure recycle compressor	MW	0.2480	2.217	6.408
-40deg.C-level refrigerating machine	MW	0.0050	0.050	0.144
Nitrogen re-liquefaction machine	MW	0.1341	1.283	3.775
Total power	MW	0.4854	4.533	13.285
Theoretical minimum power	MW	0.165	1.65	4.95
Process efficiency	%	34.0	36.4	37.3

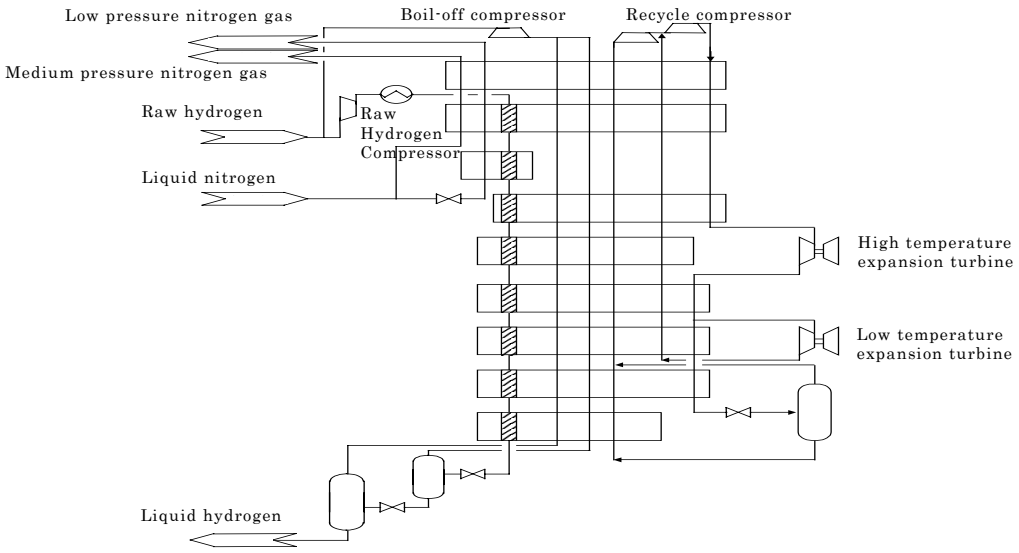

Figure 9.3.2-6. Hydrogen liquefaction process flow sheet

(2) Conditions for study

We decided to use LNG with the following composition: methane: 90.78mol%, ethane: 5.92mol%, propane: 2.39mol%, butane: 0.88mol%, pentane: 0.02mol% and nitrogen: 0.01mol%. With this composition, boiling point is -160.3℃ at atmospheric pressure and -90℃ at 3.2MPa, and dew point is -30.2℃. LNG temperature after pressurization was set at 153℃ at inlet of heat exchanger for cooling recovery. For production of H_2 from NG, combination of steam reforming, CO conversion and PSA was assumed. Although typical reforming process pressure is around 1.0-2.8MPa, 3.0MPa was selected to match the booster pressure for raw hydrogen. The following case was studied for utilizing the cryogenic heat of LNG.

Case 1: (See Figure 9.3.2-7)

After boosting the LNG by pump, its cryogenic heat is used to cool the raw hydrogen down to -150℃ in the hydrogen liquefaction machine. After that, LN_2 is used as an auxiliary coolant to cool down to 80K level. The following values were set for pressure: pump inlet: atmospheric (0.101325MPa), pump outlet: 3.3MPa, LNG/NG inside the heat exchanger: 3.2MPa, raw hydrogen inside the heat exchanger: 3.0MPa. Ortho-to-para conversion was also assumed. Excess cooling near room temperature was to be used for cooling the cooling water.

Case 2: (See Figure 9.3.2-8)

LNG cooling is also used for re-liquefaction of LN_2, which is used as an auxiliary coolant. Nitrogen is used for cycle gas to re-liquefy LN_2, and a cryogenic compressor was selected as a circulating compressor.

Case 3: (See Figure 9.3.2-9)

Furthermore, cryogenic compressor was also selected for high pressure hydrogen recycle compressor for hydrogen liquefaction machine. A separate LNG system was used for this compressor with the following pressures: pump inlet: atmospheric (0.101325MPa), pump outlet: 1.1MPa, LNG/NG inside the heat exchanger: 1.0MPa.

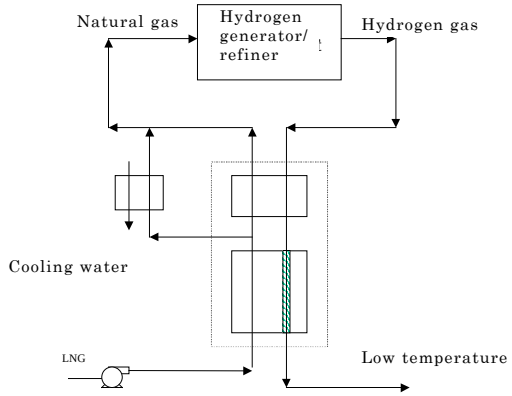

Figure 9.3.2-7. Process flow for

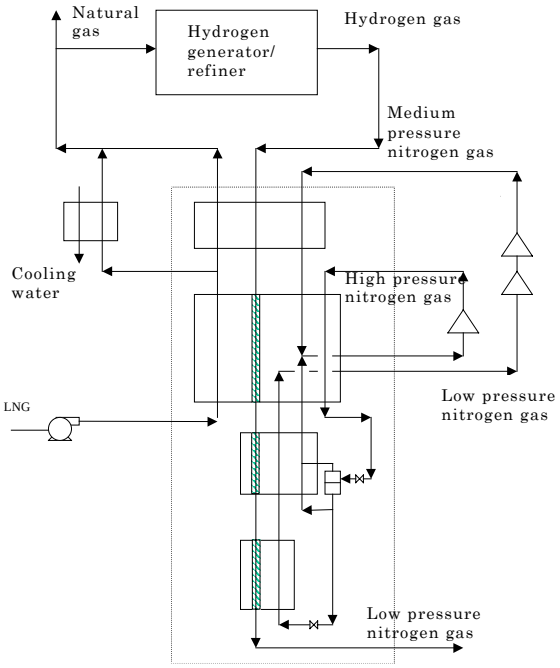

Figure 9.3.2- 8. Process flow for

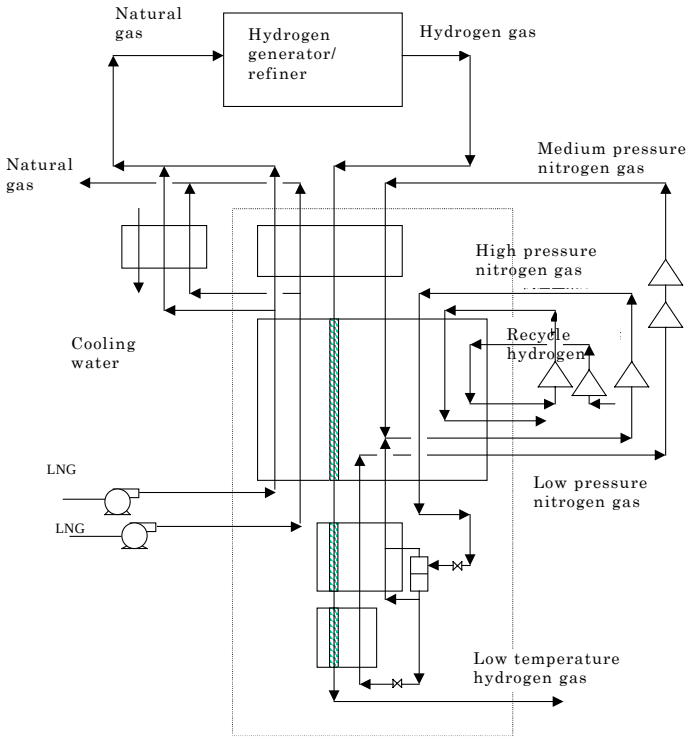

Figure 9.3.2-9. Process flow for

(3) Summary of study results

The results are shown in Table 9.3.2-3. In Case 1, required LNG volume is determined by temperature region below the boiling point of LNG, and the results indicated that 0.4555Nm3/h of LNG per 1Nm3/h of hydrogen gas was required. Since re-liquefaction of flashed hydrogen (15%) is also required in the raw hydrogen system of the hydrogen liquefaction machine, required LNG volume was determined as shown in Table 3.

In case 2, to also use LNG for re-liquefaction of nitrogen to generate auxiliary cooling, we assumed that cooling at higher than -150℃ can be obtained "free of charge" from LNG. First, optimization of power for nitrogen cycle below -150℃ was studied and it was found that high pressure of nitrogen should be higher than 2.94MPa but as low as possible.

On the other hand, it was found that required LNG volume was determined by the amount of heat required to liquefy high pressure flow of nitrogen, due to heat balance over -150℃. It was also found that required LNG volume would infinitely increase as conditions approached the optimum power conditions for the above-mentioned nitrogen cycle below -150℃. Based on the above, we conducted a study to determine the required power, where high pressure of nitrogen was 4.5MPa and a cryogenic compressor was used as circulating compressor.

In case 3, we studied a case where high pressure hydrogen recycle compressor of the hydrogen liquefaction machine was used as low temperature compressor, utilizing LNG cooling. As required volume for cooling increases, high pressure of nitrogen re-liquefaction was reduced to 3.5MPa. Since the boiling point (BP) of LNG at 1MPa is -121.5℃, we were able to lower the operating temperature of high pressure hydrogen recycle compressor, contributing to reduction of power.

(4) Comments

Case 1 shows that it is possible to substantially reduce power, as power required to boost LNG is very small. Increase in construction cost to cool the raw hydrogen down to -150℃ is negligible. Reduction in power and construction cost can also be expected.

In case 2, a realistic solution for a small facility of around 1t/d would be to omit the nitrogen re-liquefaction machine and to supply LN_2 externally by a tank lorry. If LNG cooling is not used for nitrogen re-liquefaction, one or two units of nitrogen expansion turbine and a nitrogen cold compressor will be used. Because cryogenic compressors are relatively expensive at present, overall trade-off between equipment cost power

must be considered. As the compressor becomes larger, it is expected to become more cost-effective. In case 3, further power reduction is possible if cryogenic compressor is used for high pressure hydrogen recycle compressor, utilizing LNG cooling. Based on above results, utilizing LNG cooling is very effective in reducing required power.

9.3.3 Subject in future

This year, we conducted studies on hydrogen expansion turbine for power recovery and power reduction in hydrogen liquefaction machine utilizing LNG cooling, for the purpose of further reducing the power required for compression in hydrogen compressors in a small-capacity hydrogen liquefaction facility, which we had been studying.

We now plan to conduct development of elemental technology for hydrogen compressor and hydrogen expansion turbine, validation with model tests, and detail design on technology to utilize LNG cooling, for validation of highly efficient, small-capacity liquefaction machine.

As specific items for next year, we plan to conduct performance validation of hydrogen expansion turbine for power recovery by model tests, and a more detailed study on small-capacity cryogenic compressor.

Table 9.3.2-3. Comparison of power requirements using LNG cooling

1t/d Liquefaction machine

Case		Conventional method	Case 1	Case 2	Case 3
Required power					
Raw hydrogen compression	MW	0.0850	0.0000	0.0000	0.0000
Low pressure hydrogen compression	MW	0.0133	0.0133	0.0133	0.0133
High pressure hydrogen compression	MW	0.2480	0.2480	0.2480	0.1579
－40deg.C	MW	0.0050	0.0000	0.0000	0.0000
Nitrogen re-liquefaction	MW	0.1341	0.0604	0.0137	0.0115
LNG pump	MW	0.0000	0.0005	0.0012	0.0012
Total required power	MW	0.485	0.322	0.276	0.184
Power unit requirement	KWh/Nm3	1.048	0.696	0597	0.397
Relative power	%	100	66.4	56.9	37.9
LNG volume	t/d	0	4.7	13.0	4.7+24.2

10t/d Liquefaction machine

Case		Conventional method	Case 1	Case 2	Case 3
Required power					
Raw hydrogen compression	MW	0.850	0.000	0.000	0.000
Low pressure hydrogen compression	MW	0.133	0.133	0.133	0.133
High pressure hydrogen compression	MW	2.217	2.217	2.217	1.291
－40deg.C	MW	0.050	0.000	0.000	0.000
Nitrogen re-liquefaction	MW	1.283	0.577	0.137	0.115
LNG pump	MW	0.000	0.005	0.012	0.012
Total required power	MW	4.53	2.93	2.50	1.55
Power unit requirement	KWh/Nm3	0.978	0.633	0.540	0.335
Relative power	%	100	64.7	55.2	34.2
LNG volume	t/d	0	47	130	47+242

30t/d Liquefaction machine

Case		Conventional method	Case 1	Case 2	Case 3
Required power					
Raw hydrogen compression	MW	2.550	0.000	0.000	0.000
Low pressure hydrogen compression	MW	0.408	0.408	0.408	0.408
High pressure hydrogen compression	MW	6.408	6.408	6.408	3.731
－40deg.C	MW	0.14	0.000	0.000	0.000
Nitrogen re-liquefaction	MW	3.775	1.690	0.410	0.345
LNG pump	MW	0.000	0.014	0.037	0.035
Total required power	MW	13.29	8.52	7.26	4.52
Power unit requirement	KWh/Nm3	0.955	0.613	0.522	0.325
Relative power	%	100	64.1	54.7	34.0
LNG volume	t/d	0	140	391	140+725